

Extended Network Thiocyanate- and Tetracyanoethanide-Based First-Row Transition Metal Complexes

Endrit Shurdha,[†] Saul H. Lapidus,[‡] Peter W. Stephens,[‡] Curtis E. Moore,[§] Arnold L. Rheingold,[§] and Joel S. Miller^{*†}

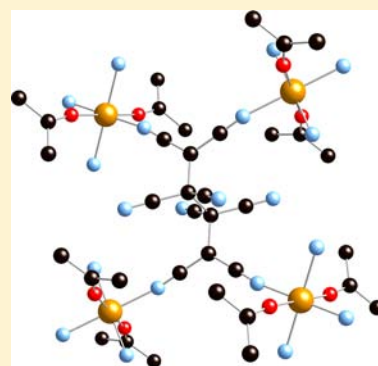
[†]Department of Chemistry, University of Utah, Salt Lake City, Utah 84112-0850, United States

[‡]Department of Physics and Astronomy, Stony Brook University, Stony Brook, New York 11794, United States

[§]Department of Chemistry, University of California, San Diego, La Jolla, California 92093-0358, United States

S Supporting Information

ABSTRACT: Linear chain thiocyanate complexes of $M(\text{NCS})_2(\text{OCMe}_2)_2$ ($M = \text{Fe}, \text{Mn}, \text{Cr}$) composition have been prepared and structurally, chemically, and magnetically characterized. $\text{Fe}(\text{NCS})_2(\text{OCMe}_2)_2$ exhibits metamagnetic-like behavior, and orders as an antiferromagnet at 6 K. The Mn and Cr compounds are antiferromagnets with T_c of 30 and 50 K, respectively, with $J/k_B = -3.5$ (-2.4 cm^{-1}) and -9.9 K (-6.9 cm^{-1}), respectively, when fit to one-dimensional (1-D) Fisher chain model ($H = -2JS_i S_j$). $\text{Co}(\text{NCS})_2$ was prepared by a new synthetic route, and powder diffraction was used to determine its structure to be a two-dimensional (2-D) layer with $\mu_{\text{N,S,S}}\text{-NCS}$ motif, and it is an antiferromagnet ($T_c = 22 \text{ K}$; $\theta = -33 \text{ K}$ for $T > 25 \text{ K}$). $M(\text{NCS})_2(\text{OCMe}_2)_2$ ($M = \text{Fe}, \text{Mn}$) and $\text{Co}(\text{NCS})_2$ react with $(\text{NBu}_4)(\text{TCNE})$ in dichloromethane to form $M(\text{TCNE})[\text{C}_4(\text{CN})_8]_{1/2}$, and in acetone to form $M[\text{C}_4(\text{CN})_8](\text{OCMe}_2)_2$ ($M = \text{Fe}, \text{Mn}, \text{Co}$). These materials possess $\mu_4\text{-}[\text{C}_4(\text{CN})_8]^{2-}$ that form 2-D layered structural motifs, which exhibit weak antiferromagnetic coupling. $\text{Co}(\text{TCNE})[\text{C}_4(\text{CN})_8]_{1/2}$ behaves as a paramagnet with strong antiferromagnetic coupling ($\theta = -50 \text{ K}$).



INTRODUCTION

Thiocyanate is a common ligand because of its versatile bonding modes.^{1,2} Thiocyanate typically bonds terminally via the nitrogen with the first row transition metals to form diverse geometries, such as $\text{V}(\text{NCS})_2\text{py}_4$ ($\text{py} = \text{pyridine}$),³ $(\text{NMe}_4)_2[\text{Fe}(\text{NCS})_4]$ ⁴ and $(\text{NEt}_4)_3[\text{Fe}(\text{NCS})_6]$ ⁴ complexes. Thiocyanate can also bridge with the M-NCS-M motif to form extended one-dimensional (1-D) and two-dimensional (2-D) structures, for example, $\text{M}(\text{NCS})_2\text{Sol}_2$ ($\text{Sol} = \text{solvent}$).⁵ Other bonding motifs include μ_3 -bridging ($>\text{SCN-}$), Table 1.⁶

Table 1. Summary of the Known Metal Coordination Modes^a of Thiocyanate Ligand⁶

<u>-NCS^a</u>	<u>-NCS^b</u>	<u>$\text{-NCS}<$</u>
<u>-SCN</u>	<u>$>\text{NCS}$</u>	<u>$>\text{NCS}<$</u>
<u>$>\text{NCS}$</u>	<u>$\text{NCS}<$</u>	<u>$\text{-NCS}\equiv$</u>

^aBold, underlined atom bonded to a metal ion; - terminal bonded; < or > μ -bonded; \equiv triply bonded.

The bonding depends on the metal ion,⁷ steric hindrance,⁸ ancillary ligands,⁹ and solvent,¹⁰ with the electronic structure and the steric hindrance being most important. π -backbonding ancillary ligands withdraw electron density from the metal disfavoring S-bound thiocyanate, for example, S-bound thiocyanate occurs for $\text{Pt}(\text{NH}_3)_2(\text{SCN})_2$ while N-bound thiocyanate is present for $\text{Pt}(\text{PEt}_3)_2(\text{NCS})_2$.¹¹ Also, lower oxidation state metals tend to form stronger S-bound thiocyanate motifs, again

because of enhanced backbonding.¹² N-bound thiocyanate forms a linear bond with a metal center, while S-bound thiocyanate forms bent M-SCN bonds.

The main diagnostic method for determining the type of bonding motif is infrared spectroscopy (IR). Free NCS^- exhibits a stretching ν_{CN} at 2054 cm^{-1} , and two δ_{NCS} bending modes at 486 and 471 cm^{-1} . Upon binding to a metal ion, the δ_{NCS} doublet typically becomes a singlet for either M-N ($\sim 480 \text{ cm}^{-1}$) or M-S bonding ($\sim 420 \text{ cm}^{-1}$).¹ The ν_{CS} frequency occurs at $\sim 800 \text{ cm}^{-1}$ and shifts either higher or lower depending on N- or S-bound thiocyanate, respectively. This frequency will not be discussed as other components, such as solvents and other ligands, mask this region. Also, the intensity of the ν_{CS} absorption is weak and occasionally is not observed.

The ν_{CN} stretch shifts above 2100 cm^{-1} for $\mu_{\text{N,S}}\text{-M-NCS-M}$ bonding.¹³ Tetrahedral or octahedral complexes with terminal thiocyanate ligands have $\nu_{\text{CN}} < 2100 \text{ cm}^{-1}$ and are dependent on the rest of the surrounding environment.¹² Also, only one δ_{NCS} bending mode is observed for tetrahedral or octahedral complexes. Compounds with the $\mu_{\text{S,S}}\text{-NCS}$ bridging motif have ν_{CN} values in the $2140\text{--}2200 \text{ cm}^{-1}$ range,¹⁴ while those with $\mu_{\text{N,N}}\text{-NCS}$ bridging have $\nu_{\text{CN}} < 2000 \text{ cm}^{-1}$.¹⁵ These shifts of the ν_{CN} are attributed to the electron delocalization from the CN triple bond.

Received: April 19, 2012

Published: August 28, 2012

A motivation for studying thiocyanate complexes is the expectation that dissociation can form free NCS^- that can reduce tetracyanoethylene^{16,17} (TCNE), and subsequently form materials with reduced TCNE, which are anticipated to exhibit magnetic ordering.^{18,19} For example, the reaction of $\text{FeCl}_2(\text{NCMe})_2$ and TCNE forms layered (2-D) $[\text{Fe}(\text{TCNE})-(\text{NCMe})_2][\text{FeCl}_4]$ that magnetically orders at 90 K.²⁰ Anticipating the ability of the SCN^- , like Cl^- , to form $[\text{FeL}_4]^{n-}$ ($n = 2, 3$; $L = \text{Cl}^-, \text{SCN}^-$), we sought to study thiocyanate complexes of the first row transition metals and their subsequent reactions with TCNE.

EXPERIMENTAL SECTION

Anhydrous metal(II) chlorides (Strem Chemicals) and KSCN (Sigma-Aldrich) were used as purchased. $[\text{M}^{\text{II}}(\text{NCMe})_6](\text{BF}_4)_2$ ($M = \text{Fe}, \text{Co}$) and $\text{M}(\text{NCMe})_4(\text{BF}_4)_2$ ($M = \text{Cr}, \text{Mn}$) were prepared as described in the literature from metal(II) chlorides and AgBF_4 (Oakwood Products).²¹ Tetracyanoethylene (TCNE) (TCI America) was sublimated to further purify the product. $(\text{NBu}_4)(\text{TCNE})$ was prepared as described in the literature.²² All syntheses were performed under dry N_2 atmosphere in Vacuum Atmosphere DriLab (<1 ppm O_2). Acetonitrile was purified through an activated alumina dual-column purification system under a positive pressure of dry N_2 . Diethyl ether (Et_2O) and acetone (Me_2CO) were distilled from appropriate drying agents under dry N_2 .

$\text{Fe}(\text{NCS})_2(\text{OCMe}_2)_2$, 1. $[\text{Fe}(\text{NCMe})_6](\text{BF}_4)_2$ (400 mg, 0.84 mmol), and KSCN (164 mg, 1.68 mmol) were each dissolved in 5 mL of acetone, and the latter was quickly added to the former solution. White KBF_4 immediately precipitated, and after stirring overnight it was removed via filtration through Celite. The light yellow solution was taken to dryness (Yield 133 mg, 83%). Compound 1 was redissolved in small amount of acetone, and diffusion of Et_2O led to formation of light yellow crystals. IR (KBr): ν_{CH} 2914 (w), ν_{CN} 2107 (s), ν_{CO} 1681 (s), $\nu_{\text{Me}_2\text{CO}}$ 1356 (m, b), 1238 (m), 1093 (m), 540 (m), δ_{NCS} 474 (m) and 426 (w) cm^{-1} . The diamagnetic correction is 143×10^{-6} emu/mol.

$\text{Mn}(\text{NCS})_2(\text{OCMe}_2)_2$, 2. $\text{Mn}(\text{NCMe})_4(\text{BF}_4)_2$ (500 mg, 1.3 mmol) and KSCN (246 mg, 2.54 mmol) were each dissolved in 5 mL of acetone, and the latter was quickly added to the former immediately precipitating KBF_4 . After stirring overnight, the mixture was filtered through Celite to remove the precipitate, and the filtrate was taken to dryness (Yield 187.5 mg, 78%). Compound 2 was redissolved in small amount of acetone, and diffusion of Et_2O led to formation of light yellow crystals. IR (KBr): ν_{CH} 2910 (w), ν_{CN} 2124 (sh), 2101 (s), ν_{CO} 1685 (s), $\nu_{\text{Me}_2\text{CO}}$ 1415 (m), 1237 (m), δ_{NCS} 478 (w) and 412 (w) cm^{-1} . The diamagnetic correction is 144×10^{-6} emu/mol.

$\text{Cr}(\text{NCS})_2(\text{OCMe}_2)_2$, 3. $[\text{Cr}(\text{NCMe})_4](\text{BF}_4)_2$ (200 mg, 0.51 mmol) and KSCN (99.7 mg, 1.02 mmol) were each dissolved in 5 mL of acetone, and the latter was quickly added to former. White KBF_4 immediately precipitated, and after stirring overnight it was removed via filtration through Celite. The light blue solution was taken to dryness forming a lime green solid (Yield 95.2 mg, 82%). Compound 3 was redissolved in a small amount of acetone, and diffusion of Et_2O led to formation of light green crystals. IR (KBr): ν_{CH} 2913 (w), ν_{CN} 2093 (s), ν_{CO} 1676 (s), $\nu_{\text{Me}_2\text{CO}}$ 1415 (m), 1357 (m), 1244 (s), δ_{NCS} 477 (w), 426 (w) cm^{-1} . The diamagnetic correction is 144×10^{-6} emu/mol.

$\text{Co}(\text{NCS})_2$, 4. $[\text{Co}(\text{NCMe})_6](\text{BF}_4)_2$ (1.00 g, 2.1 mmol) and KSCN (99.7 mg, 1.02 mmol) were each dissolved in 10 mL of acetone, and the latter was quickly added to the former. White KBF_4 immediately precipitated, and after stirring overnight it was removed via filtration through Celite. The blue solution was taken close to dryness, and Et_2O was added to precipitate the brown product (Yield 343 mg, 81%). Suitable single crystals were not obtained, but powder X-ray diffraction (XRD) analysis and Rietveld refinement were performed to determine its structure. IR (KBr): ν_{CN}

Table 2. Key IR Absorptions and Color for Compounds 1 to 11

compound	M^{II}	ν_{CN} (cm^{-1})	ν_{CO} (cm^{-1}) [Me_2CO]	δ_{NCS} (cm^{-1}) M-N	δ_{NCS} (cm^{-1}) M-S	color
1	Fe	2107 (s)	1681 (s)	474 (m)	426 (m)	yellow
2	Mn	2124 (sh), 2101 (s)	1685 (s)	478 (m)	412 (m)	yellow
3	Cr	2093 (s)	1676 (s)	477 (m)	426 (m)	green
4	Co	2154 (s)		454 (m)		brown
5	Fe	2222 (s), 2174 (s)				brown
6	Mn	2224 (s), 2183 (s), 2173 (s)				green
7	Co	2229 (s), 2189 (s), 2173 (s)				black
8	Fe	2217 (s), 2162 (s)	1697 (s)			tan
9	Mn	2222 (s), 2170 (s)	1697 (s)			white
10	Co	2228 (s), 2176 (s)	1701 (s)			tan
11	Co	2309 (w), 2283 (w), 2224 (s), 2162 (s)				brown

2154 (s), δ_{NCS} 454 (w) cm^{-1} . The diamagnetic correction is 74×10^{-6} emu/mol.

$\text{Fe}(\text{TCNE})[\text{C}_4(\text{CN})_8]_{1/2} \cdot z\text{CH}_2\text{Cl}_2$, 5. **1** (150 mg, 0.52 mmol) was suspended in 10 mL of CH_2Cl_2 , and $(\text{NBu}_4)(\text{TCNE})$ (386 mg, 1.041 mmol) was dissolved in 10 mL of CH_2Cl_2 . The latter solution was added to the suspension of **1**, and stirred for 5 days. The orange mixture turned to dark brown, and it was filtered through a fritted funnel. The dark brown precipitate was washed twice with small amounts of CH_2Cl_2 and allowed to dry under vacuum (Yield 81 mg, 82%). Powder XRD analysis confirmed that the compound was identical to that previously reported.²³ IR (KBr): ν_{CN} 2222 (s), 2174 (s) cm^{-1} . The diamagnetic correction is 133×10^{-6} emu/mol. A TGA analysis has $z = 0.59$.

$\text{Mn}(\text{TCNE})[\text{C}_4(\text{CN})_8]_{1/2} \cdot z\text{CH}_2\text{Cl}_2$, 6. **2** (75 mg, 0.26 mmol) was suspended in 10 mL of CH_2Cl_2 , and $(\text{NBu}_4)(\text{TCNE})$ (195 mg, 0.52 mmol) was dissolved in 10 mL of CH_2Cl_2 . The latter solution was to the suspension of **2**, and stirred for 5 days. The orange mixture turned to dark green, and it was filtered through a fritted funnel. The dark green precipitate was washed twice with small amounts of CH_2Cl_2 and allowed to dry under vacuum (Yield 83 mg, 85%). Powder XRD analysis confirmed that the compound was identical to that previously reported.²⁴ IR (KBr): ν_{CN} 2224 (s), 2183(s), 2173 (s) cm^{-1} . The diamagnetic correction is 134×10^{-6} emu/mol. A TGA analysis has $z = 1.01$.

$\text{Co}(\text{TCNE})[\text{C}_4(\text{CN})_8]_{1/2} \cdot z\text{CH}_2\text{Cl}_2$, 7. **4** (50 mg, 0.29 mmol) was suspended in 10 mL of CH_2Cl_2 , and $(\text{NBu}_4)(\text{TCNE})$ (212 mg, 0.57 mmol) was dissolved in 10 mL of CH_2Cl_2 . The latter solution was added to a suspension of **4**, and stirred for 5 days. The orange mixture turned to black, and it was filtered through a fritted funnel. The black precipitate was washed twice with small amounts of CH_2Cl_2 and allowed to dry under vacuum (Yield 62 mg, 60%). Powder XRD analysis and Rietveld refinement were performed to determine its structure. IR (KBr): ν_{CN} 2229 (s), 2189 (s), 2173 (s) cm^{-1} . The diamagnetic correction is 132×10^{-6} emu/mol. A TGA analysis has $z = 0.82$.

$\text{Fe}[\text{C}_4(\text{CN})_8](\text{OCMe}_2)_2$, 8. **1** (150 mg, 0.52 mmol) and $(\text{NBu}_4)(\text{TCNE})$ (386 mg, 1.04 mmol) were each dissolved in 10 mL of acetone. The latter solution was added to the solution of **1**, and an immediate orange-brown mixture formed. After being stirred overnight the mixture turned to green, and it was filtered through a fritted funnel. A light tan precipitate was obtained (Yield 86 mg, 38%). Suitable single crystals were not obtained, but powder XRD analysis and

Table 3. Summary of the Crystallographic Parameters for Compounds 1 to 11

compound	1	2	3	4	5	6	7	8	9	10	11
empirical formula	Fe ^{II} (NCS) ₂ (OCMe ₂) ₂	Mn ^{II} (NCS) ₂ (OCMe ₂) ₂	C ^{IV} (NCS) ₂ (OCMe ₂) ₂	Co(NCS) ₂	Fe(TCNE)[C ₄ (CN) ₈] _{0.5}	Mn(TCNE)[C ₄ (CN) ₈] _{0.5}	Co(TCNE)[C ₄ (CN) ₈] _{0.5}	Fe[C ₄ (CN) ₈](OCMe ₂) ₂	Mn[C ₄ (CN) ₈](OCMe ₂) ₂	Co[C ₄ (CN) ₈](OCMe ₂) ₂	Co[C ₄ (CN) ₈](NCMe) ₂
MW, g/mol	288.17	287.26	284.32	175.10	312.03 ^a	311.12 ^a	315.13 ^a	428.21	427.30	431.29	397.238
T (K)	100(2)	296(2)	121(2)	295	298	298	295	295	295	295	295
a (Å)	5.7215(8)	5.798(9)	5.734(4)	10.5959(3)	14.3172(2)	14.4317(7)	14.2343(5)	7.8809(3)	7.8212(2)	7.9191(2)	7.5754(2)
b (Å)	7.6941(11)	7.868(10)	7.769(5)	3.72504(11)	17.4017(3)	17.5615(1)	17.2526(10)	11.4483(5)	11.6487(3)	11.5882(3)	11.4839(3)
c (Å)	7.8456(12)	8.027(12)	7.820(5)	6.16597(19)	7.3334(1)	7.4864(5)	7.2908(3)	11.5662(4)	11.6871(3)	11.4825(3)	11.1083(3)
α (deg)	109.864(2)	110.70(3)	107.905(9)	90	90.00	90.00	90.00	90.00	90.00	90.00	90.00
β (deg)	99.983(2)	99.119(16)	99.027(9)	105.862(3)	90.00	90.00	90.00	100.146(4)	99.055(3)	100.558(3)	107.101(3)
γ (deg)	97.286(2)	97.90(3)	98.315(9)	90	90.00	90.00	90.00	90.00	90.00	90.00	90.00
V (Å ³)	313.41(8)	330.7(8)	320.4(4)	234.106(12)	1827.07	1897.36	1790.46(14)	1027.21(7)	1051.51(5)	1018.00(5)	923.65(4)
Z	1	1	1	2	2	2	2	2	2	2	2
space group	P $\bar{1}$	P $\bar{1}$	P $\bar{1}$	C2/m	Cmmm	Cmmm	Cmmm	P2 ₁ /c	P2 ₁ /c	P2 ₁ /c	P2 ₁ /c
ρ _{calc} (g cm ⁻³)	1.527	1.442	1.473	2.484				1.384	1.350	1.407	1.428
R1 [I > 2σ(I)] ^b	0.0278	0.0649	0.0295	0.69994	0.70247	0.69733	0.70012	0.69938	0.69951	0.70003	0.69919
wR2 [I > 2σ(I)] ^c	0.0719	0.1883	0.0765								
R _{exp} ^{d,e}				0.0774			0.0465	0.0298	0.0429	0.0456	0.0457
R _{exp} ^f				0.0593			0.0376	0.0145	0.0260	0.0285	0.0274
goodness of fit	0.997	1.135	1.041	1.304			1.235	2.058	1.649	1.600	1.668
largest diff. peak/hole, e ⁻ Å ⁻³			0.291								
CCDC#	806641	806645	806647	876943	623463	745885	876944	876945	876946	876947	876948

^aExcludes the solvent. ^bR₁ = Σ||F_o - |F_c|| / Σ|F_o|. ^cwR₂ = [Σw(F_o² - F_c²)² / Σw(F_o²)]^{1/2}. ^dR_{WP} = ((Σw_i(y_i^{calc} - y_i^{obs})²) / (Σw_i(y_i^{obs})²))^{1/2}. ^ey_i^{calc} and y_i^{obs} are the calculated and observed intensities at the ith point in the profile, normalized to monitor intensity. The weight w_i is 1/σ² from the counting statistics, with the same normalization factor. N is the number of points in the measured profile minus number of parameters. ^fR_{exp} = (N / (Σw_i(y_i^{obs})²))^{1/2}.

Rietveld refinement were performed to determine its structure. IR (KBr): ν_{CN} 2217 (s), 2162 (s), ν_{CO} 1697 (s) cm^{-1} . The diamagnetic correction is 199×10^{-6} emu/mol.

Mn[C₄(CN)₈](OCMe₂)₂, 9. 2 (150 mg, 0.52 mmol) and (NBu₄)-(TCNE) (386 mg, 1.04 mmol) were each dissolved in 10 mL of acetone. The latter solution was added to the solution of **2**, stirred overnight, and an orange mixture formed. After a few minutes it was filtered through a fritted funnel. A white precipitate was obtained (Yield 43 mg, 19%). Powder XRD analysis and Rietveld refinement were performed to determine its structure. IR (KBr): ν_{CN} 2222 (s), 2170 (s), ν_{CO} 1697 (s) cm^{-1} . The diamagnetic correction is 200×10^{-6} emu/mol.

Co[C₄(CN)₈](OCMe₂)₂, 10. 4 (30 mg, 0.17 mmol) and (NBu₄)-(TCNE) (127 mg, 0.34 mmol) were each dissolved in 10 mL of acetone. The latter solution was added to the solution of **4**, stirred overnight, and an immediate green mixture formed. Upon filtration through a fritted funnel a light tan precipitate was obtained (Yield 20 mg, 27%). Powder XRD analysis and Rietveld refinement were performed to determine its structure. IR (KBr): ν_{CN} 2228 (s), 2176 (s), ν_{CO} 1701 (s) cm^{-1} . The diamagnetic correction is 199×10^{-6} emu/mol.

Co[C₄(CN)₈](NCMe)₂, 11. CoI₂(NCMe)₂ (50 mg, 0.13 mmol) and was dissolved in 5 mL of acetonitrile, and it was added to a 5 mL acetonitrile solution of TCNE (50 mg, 0.39 mmol). Upon mixing an immediate color change to dark brown occurred. The reaction was stirred for 3 days and filtered through a fritted funnel to collect a light brown precipitate (Yield 34 mg, 66%). Powder XRD analysis and Rietveld refinement were performed to determine its structure. IR (KBr): ν_{CN} 2309 (w), 2283 (w), 2224 (s), 2162 (s). The diamagnetic correction is 187×10^{-6} emu/mol.

Physical Measurements. Infrared spectra were recorded from 400 to 4000 cm^{-1} on a Bruker Tensor 37 infrared spectrophotometer ($\pm 1 \text{ cm}^{-1}$) with a KBr pellet. Thermogravimetric analyses (TGA) with mass spectroscopic (MS) analysis of the gaseous products were performed with a TA Model Q500 TGA equipped with a Pfeiffer Thermostar GSD301T3 quadrupole mass spectrometer to identify gaseous products with masses less than 300 amu. Experiments were performed in a Vacuum Atmospheres DriLab under nitrogen to protect air- and moisture-sensitive samples. Samples were placed in an aluminum pan and heated at 5 $^{\circ}\text{C}/\text{min}$ under a continuous 10-mL/min-nitrogen flow.

Magnetic susceptibility measurements were made between 5 and 300 K using a Quantum Design MPMS-5 ST SQUID magnetometer with a sensitivity of 10^{-8} emu or 10^{-12} emu/Oe at 1T and equipped with the ultralow field (~ 0.005 Oe), reciprocating sample measurement system, and continuous low temperature control with enhanced thermometry features, as previously reported.²⁵ Diamagnetic corrections were made using Pascal's constants. Small amounts of ferromagnetic impurities are ubiquitous²⁶ and were sometimes evident from $\chi T(T)$ increasing at higher temperature, and the amount of iron at the ppm level was determined from that needed to reach constant $\chi T(T)$ values.

The single crystal structures of **1**, **2**, and **3** were determined on a Nonius KappaCCD diffractometer equipped with Mo $K\alpha$ radiation. All the reflections were merged, and only those for which $I_0 > 2\sigma(I)$ were included in the refinement, where $\sigma(F_o)^2$ is the standard deviation based on counting statistics. The data for compounds **1**, **2**, and **3** were integrated using the Bruker SAINT software program.²⁷ The structures were solved by a combination of direct methods and heavy atom methods. Patterson methods and the refinement by full-matrix least-squares methods using SHELXL-97 were used for the structures of **1**, **2**, and **3**. All the non-hydrogen atoms were refined with anisotropic displacement coefficients. Hydrogen atoms were assigned isotropic displacements $U(\text{H}) = 1.2U(\text{C})$, and their coordinates were allowed to ride on their respective carbons using SHELXL97.²⁸

High resolution powder diffraction measurements for Rietveld structure analysis for compounds **4** and **7** to **11** were performed at Beamline X16C of the National Synchrotron Light Source at Brookhaven National Laboratory. The powdered samples were held in a 1.0 mm diameter thin-wall quartz capillaries. X-rays of a single

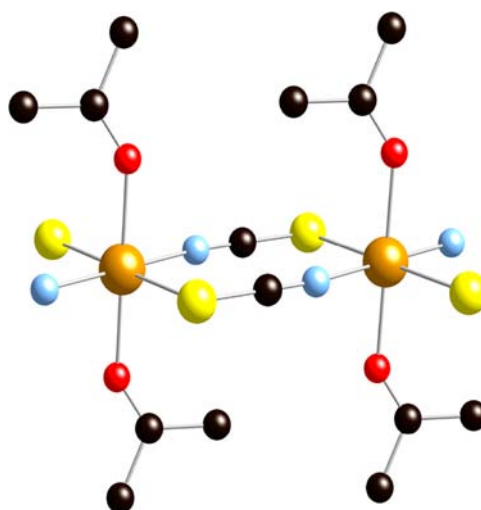


Figure 1. Structure of $\text{Fe}(\text{NCS})_2(\text{OCMe}_2)_2$ (**1**); hydrogen atoms are omitted for clarity.

Table 4. $\angle\text{MNC}$, $\angle\text{NCS}$, and $\angle\text{CSM}$ within Compounds **1** to **4**

compound	$\angle\text{MNC}$, deg	$\angle\text{NCS}$, deg	$\angle\text{CSM}$, deg
1	165.45	180	101.76
2	165.92	180	100.88
3	169.47	178.63	97.60
4	163.40	176.49	101.41
$\text{Fe}(\text{NCS})_2(\text{py})_2$ ³⁹	164.79	180	99.49
$\text{Ni}(\text{NCS})_2$ ³⁸	161.67	178.25	100.88

wavelength were selected by a Si(111) channel cut crystal. Diffracted X-rays were selected by a Ge(111) analyzer and detected by a NaI scintillation counter. The capillary was spun at several Hz during data collection to improve particle statistics. The incident intensity was monitored by an ion chamber and used to normalize the measured signal. The TOPAS-Academic program was used to index, solve, and refine the crystal structures.^{29–31} Rietveld plots are given in the Supporting Information.

RESULTS AND DISCUSSION

The reaction of $[\text{M}(\text{NCMe})_x](\text{BF}_4)_2$ [$\text{M} = \text{Fe}, \text{Mn}, \text{Cr}; x = 6$ (Fe, Co), 4 (Mn, Cr)] and 2 equiv of KSCN in acetone formed $\text{M}(\text{NCS})_2(\text{OCMe}_2)_x$ [$x = 2$ for Fe (**1**), Mn (**2**), Cr (**3**), $x = 0$ for Co (**4**)]. Each has ν_{CN} absorptions above 2100 cm^{-1} (2107, 2101, and 2154 cm^{-1} for **1**, **2**, and **4**, respectively), indicative of bridging thiocyanates, while **3** has a ν_{CN} at 2093 cm^{-1} . Albeit slightly below 2100 cm^{-1} **3** has $\mu_{\text{N,S}}\text{-NCS}$ that is ascribed to weaker interaction between the $\text{Cr}(\text{II})$ ion and the thiocyanate sulfur.¹²

Two additional IR absorptions support the bridging thiocyanate motif; δ_{NCS} (474, 478, and 477 cm^{-1} , respectively) for the M-N bond and δ_{NCS} (426, 412, and 426 cm^{-1} , respectively) for the M-S bond for **1**, **2**, and **3**. Compound **4** has only one δ_{NCS} at 454 cm^{-1} indicative of a M-N bond, but no M-S δ_{NCS} is observed. Coordinated acetone is evident from the observed ν_{CO} absorptions at 1681, 1685, and 1676 cm^{-1} for **1**, **2**, and **3**, respectively, which occur at lower frequency with respect to uncoordinated acetone at 1720 cm^{-1} . Dissolution of **4** in MeCN forms $[\text{Co}^{\text{II}}(\text{NCMe})_5\text{Co}^{\text{II}}(\text{NCS})_4]\cdot\text{MeCN}$.³²

Redox reactions of the aforementioned thiocyanate complexes with TCNE were unsuccessful. Akin to iodide, thiocyanate should be reduced by TCNE to form $[\text{TCNE}]^{\bullet-}$;

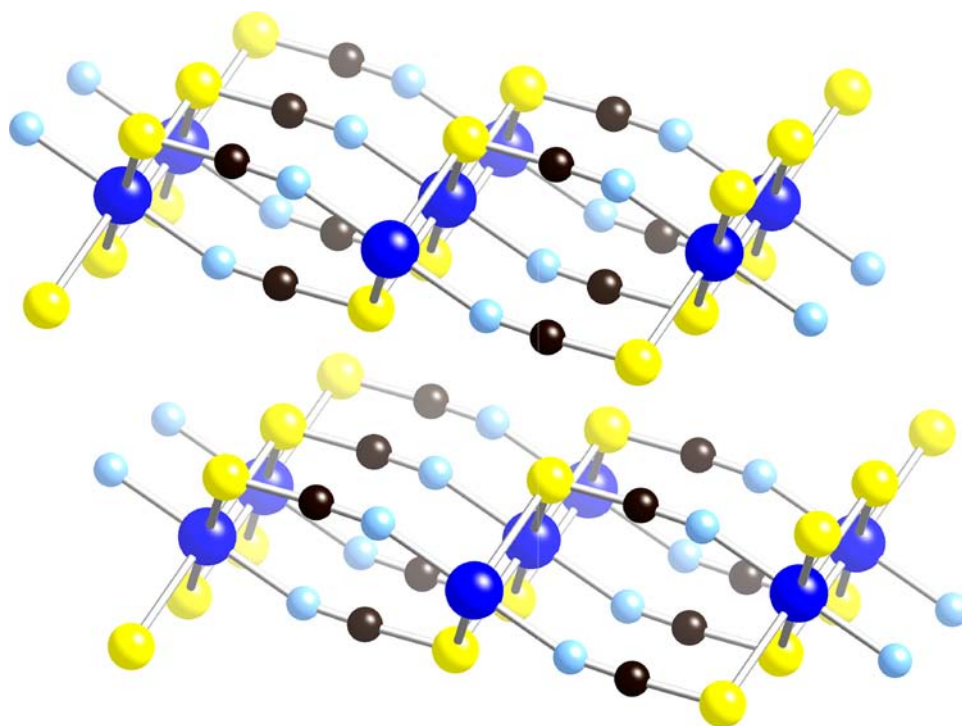


Figure 2. 2-D Structure of $\text{Co}(\text{NCS})_2$ (**4**) with $\mu_{\text{N,S,S}'}$ -NCS bound to Co centers.

however, this did not occur. This is attributed to the lack of dissociation of metal-bound thiocyanate, and thus none was available for this reaction. The aforementioned $[\text{Co}^{\text{II}}(\text{NCMe})_5\text{Co}^{\text{II}}(\text{NCS})_4]$, however, did react via substitution with $[\text{TCNE}]^{\bullet-}$.

$\text{M}(\text{TCNE})[\text{C}_4(\text{CN})_8]_{1/2} \cdot z\text{CH}_2\text{Cl}_2$ ($z = 0.3\text{--}1.5$), Fe (**5**), Mn (**6**), 6 Co (**7**), were prepared by reacting **1**, **2**, and **4** with 2 equiv of $(\text{NBu}_4)(\text{TCNE})$ in CH_2Cl_2 for 5 days. The reaction of **3** with $(\text{NBu}_4)(\text{TCNE})$, however, yields an unknown product. Compounds **5** and **6** have been previously prepared via redox chemistry of metal carbonyl and TCNE ($\text{M} = \text{Fe}$),³³ or $\text{Ml}_2 \cdot z\text{NCMe}$ ($\text{M} = \text{Mn}, \text{Fe}$) and TCNE,³⁴ and were structurally characterized.^{23,24} The new synthetic route identified herein employs a ligand exchange between thiocyanate and $[\text{TCNE}]^{\bullet-}$ and has not been previously reported. These three compounds have similar ν_{CN} frequencies at 2222 and 2174 cm^{-1} for **5**, 2224, 2183, and 2173 cm^{-1} for **6**, and 2229, 2189, and 2173 cm^{-1} for **7**. These frequencies are characteristic of metal bound $[\text{TCNE}]^{\bullet-}$.¹⁷

$\text{M}[\text{C}_4(\text{CN})_8](\text{OCMe}_2)_2$ [$\text{M} = \text{Fe}$ (**8**), Mn (**9**), Co (**10**)] was prepared by reacting compounds **1**, **2**, and **4** with 2 equiv of $(\text{NBu}_4)(\text{TCNE})$ in acetone overnight. They have ν_{CN} frequencies at 2217 and 2162 cm^{-1} for **8**, 2222 and 2170 cm^{-1} for **9**, 2228 and 2176 cm^{-1} for **10**. The ν_{CO} frequencies at 1697, 1697, and 1701 cm^{-1} for **8**, **9**, and **10** suggest coordinated acetone. $\text{Co}[\text{C}_4(\text{CN})_8](\text{NCMe})_2$, **11**, was prepared from $\text{CoI}_2(\text{NCMe})_2$ and TCNE in acetonitrile, and has four peaks in the CN region. The first two at 2309 and 2283 cm^{-1} correspond to coordinated acetonitrile and the other two at 2224 and 2162 cm^{-1} correspond to coordinated $[\text{C}_4(\text{CN})_8]^{2-}$. A summary of all the diagnostic peaks for compounds **1** to **11** is shown in Table 2.

Structures. The structures of **1**, **2**, and **3** were determined by single crystal X-ray analyses, and a summary of key crystallographic parameters are provided in Table 3. **1**, **2**, and **3** were determined to be $\text{M}(\text{NCS})_2(\text{OCMe}_2)_2$ ($\text{M} = \text{Fe}, \text{Mn}, \text{Cr}$), and

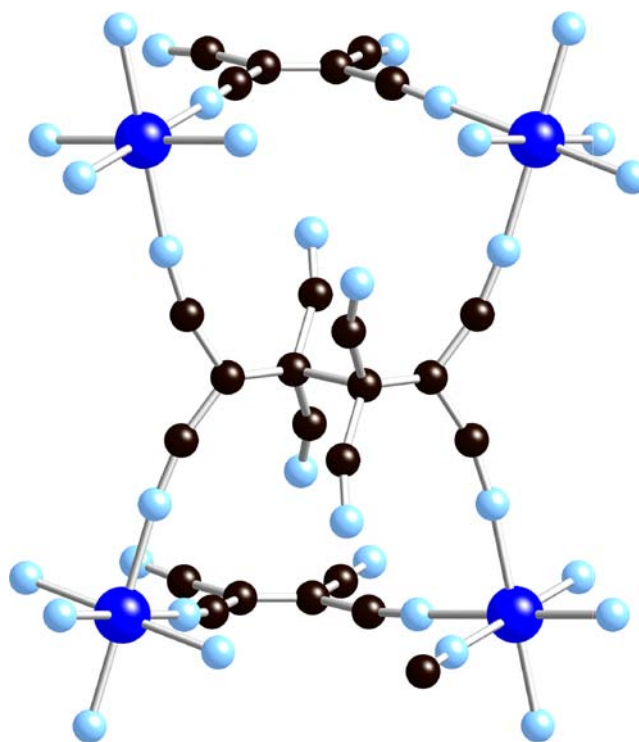


Figure 3. Structure of $\text{Co}(\text{TCNE})[\text{C}_4(\text{CN})_8]_{1/2}$ (**7**). The orientational disorder present for $\mu_4\text{-}[\text{C}_4(\text{CN})_8]^{2-}$ is not shown.

are isostructural. These structures possess octahedral M^{II} centers coordinated with two *trans*-N-bound and two S-bound thiocyanate ligands in the equatorial position, forming linear chains with *trans*-acetone ligands bound to the M^{II} s above and below the plane (Figure 1 for $\text{M} = \text{Fe}$). Acetone coordinating complexes are uncommon,³⁵ as acetone is a very weak ligand. Recent studies have shown similar 1-D thiocyanate bridged chains

Table 5. Selected Atomic Distances for Compounds μ_4 -[C₄(CN)₈]²⁻

compound	M–N _{equ}	M–N _{ax}	M–O	M···M _{intra}	M···M _{inter}	C ₁ –C ₁ ^a	C ₁ –C ₂ ^b	C–N
5 ²³	2.184(3)	2.161(6)		7.1586(1)	8.7008(1)	1.586(18)	1.523(17)	1.11(1)
6 ²⁴	2.242(8)	2.209(10)		7.2158(3)	8.7808(5)	1.634(30)	1.463(27)	1.126(15)
7	2.123(5)	2.073(7)		7.1171(3)	8.6263(5)	1.648(18)	1.452(8)	1.189(5)
8	2.077(6)		2.115(7)	8.1370(2)	7.8809(3)	1.624(7)	1.584(5)	1.128(6)
9	2.128(5)		2.183(5)	8.2505(1)	7.8212(2)	1.536(5)	1.584(4)	1.157(6)
10	2.042(5)		2.073(4)	8.0861(1)	7.9191(2)	1.606(6)	1.584(5)	1.157(7)
11	2.072(3)	2.103(4)		7.9887(1)	7.5754(2)	1.563(9)	1.467(7)	1.120(6)
Fe[C ₄ (CN) ₈](NCMe) ₂ ⁴⁰	2.221(6)	2.273(6)		7.562(1)	9.356(1)	1.626(9)	1.509(9)	1.139(12)
Fe[C ₄ (CN) ₈](NCMe) ₂ ⁴¹	2.115(3)	2.186(4)		8.127(1)	8.060(1)	1.655(8)	1.508(9)	1.132(4)
Mn[C ₄ (CN) ₈](NCMe) ₂ ⁴⁰	2.218(4)	2.235(5)		7.581(1)	7.626(1)	1.646(17)	1.596(11)	1.140(6)
Mn(TPyA)[C ₄ (CN) ₈] _{1/2} ClO ₄ ⁴²	2.130(3)	2.244(3)		8.327	8.066	1.604(8)	1.611(8)	1.142(4)

^aCentral C–C bond for [C₄(CN)₈]²⁻. ^bDistance between a central carbon and CN.

prepared from the removal of pyridine (py),³⁶ and 2,2'-bipyridine (bipy)³⁷ by thermolysis, that is, M(NCS)₂(py)₄ (M = Fe, Mn, Co, Ni) or Fe(NCS)₂(bipy)₂ were converted to 1-D chains of M(NCS)₂(py)₂ and Fe(NCS)₂bipy composition.

The M–N bond lengths vary between 2.093(3) Å (Fe), 2.037(10) Å (Cr), and 2.135(28) Å (Mn). The M–O bond lengths are 2.154(2), 2.249(4), and 2.073(2) Å, and the M–S bond lengths are 2.5785(6), 2.678(3), and 2.874(24) Å for **1**, **2**, and **3**, respectively. It is interesting to note that the M–S bond length increases from iron to chromium by ~0.3 Å. This difference can be attributed to the decrease of the d-electrons between the metal centers, where more d-electrons present in the metal center facilitate stronger M–S bond in thiocyanate complexes.¹² The intrachain M···M separations are essentially identical for M = Fe (5.721 Å), Mn (5.798 Å), and Cr (5.734 Å), as are the shortest interchain M···M distances of Fe (7.694 Å), Mn (7.868 Å), and Cr (7.769 Å).

The ∠MNC, ∠NCS, and ∠CSM for **1–3** are comparable to each other and range from 165.5° to 169.5°, 178.6°–180°, and 97.6°–101.8°, respectively, Table 4. These values are in accord with that reported of 164.8°, 180°, and 99.5°, respectively, for Fe(NCS)₂(py)₂.³⁹ There is no correlation between the IR values and bond angles for these compounds.

Compound **4** was determined to be Co(NCS)₂. This compound was prepared similar to the **1–3**, but acetone was not present to form the chains. Albeit known, to the best of our knowledge the structure and/or magnetic properties have yet to be reported for Co(NCS)₂.

Each octahedral Co(II) has four bridging sulfur atoms and two bridging nitrogen atoms, and has μ_{N,S,S}-NCS (-NCS<) ligand (Figure 2). The structure consists of stacked 2-D planes, and it is isostructural to Ni(NCS)₂.³⁸ The Co–N bond length is 2.032(5) Å, while the Co–S bond length is 2.577(2) Å. There are two intralayer Co···Co distances of 3.725 and 5.616 Å, and the shortest interlayer Co···Co distance is 6.166 Å. Similarly, **4** has ∠MNC, ∠NCS, and ∠CSM of 163.4°, 176.5°, and 101.4° that are expected for a μ_{N,S,S}-thiocyanate complex, and are similar to Ni(NCS)₂ (Table 4).³⁸ Again, there is no correlation between the IR absorption frequencies and bond angles for these compounds.

Compounds **5–7** were determined to be M(TCNE)-[C₄(CN)₈]_{1/2}·zCH₂Cl₂ (M = Fe (**5**), Mn (**6**), Co (**7**); z = 0.3–1.5). These isostructural compounds consist of octahedral M(II) centers coordinated to μ₄-[TCNE]^{•-} forming a corrugated layer, which are connected by μ₄-[C₄(CN)₈]²⁻ dimers to form a 3-D structure (Figure 3). The central structure within the μ₄-[C₄(CN)₈]²⁻ is orientationally disordered,

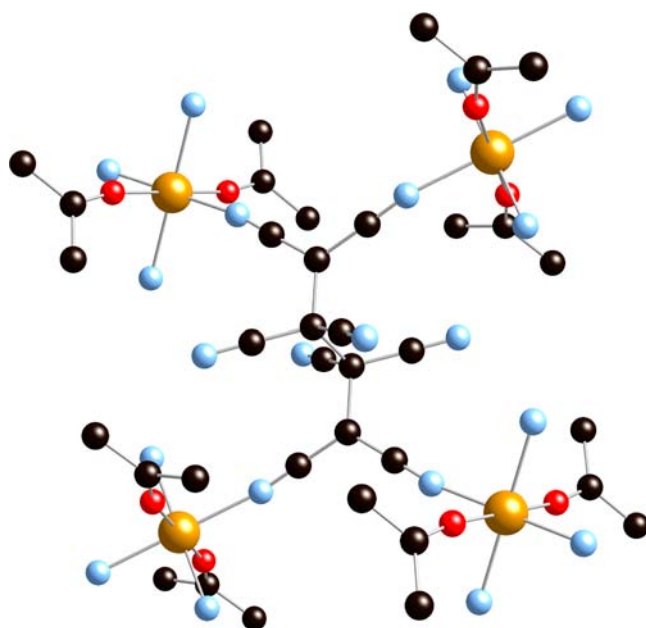


Figure 4. Structure of Fe[C₄(CN)₈](OCMe₂)₂ (**8**). The orientational disorder present for μ₄-[C₄(CN)₈]²⁻ is not shown.

and the associated atoms have a 50% occupancy, as previously reported for related compounds possessing μ₄-[C₄(CN)₈]²⁻.^{23,24,40,41} The CH₂Cl₂ solvent in **7** is disordered similar to what has been observed in **5** and **6**.^{23,24} In the structural refinements it was modeled by several effective atoms with large thermal parameters located inside the solvent-accessible cavities of the structure. Compounds **5** and **6** have been previously reported^{23,24} while **7** has been elusive. The Co–N bond length is 2.123(5) Å for the μ₄-[TCNE]^{•-} in the equatorial direction and 2.073(7) Å for the μ₄-[C₄(CN)₈]²⁻ dimer in the axial positions. These bond lengths are slightly shorter when compared with **5** and **6**. The intralayer Co···Co distance is 7.1171(3) Å and interlayer distance of 8.6263(5) Å. A summary of selected average atomic distances for compounds **5** to **11** and relevant comparison compounds are shown in Table 5.

M[C₄(CN)₈](OCMe₂)₂ [M = Fe (**8**), Mn (**9**), Co (**10**)] are isostructural and have an octahedral M^{II} bound to μ₄-[C₄(CN)₈]²⁻, forming 2-D layers. Acetones are coordinated in the axial positions, capping the octahedral centers (Figure 4). Similar to **5–7**, the μ₄-[C₄(CN)₈]²⁻ is an orientationally disordered in **8–11**. Each has two sets of M–N bond

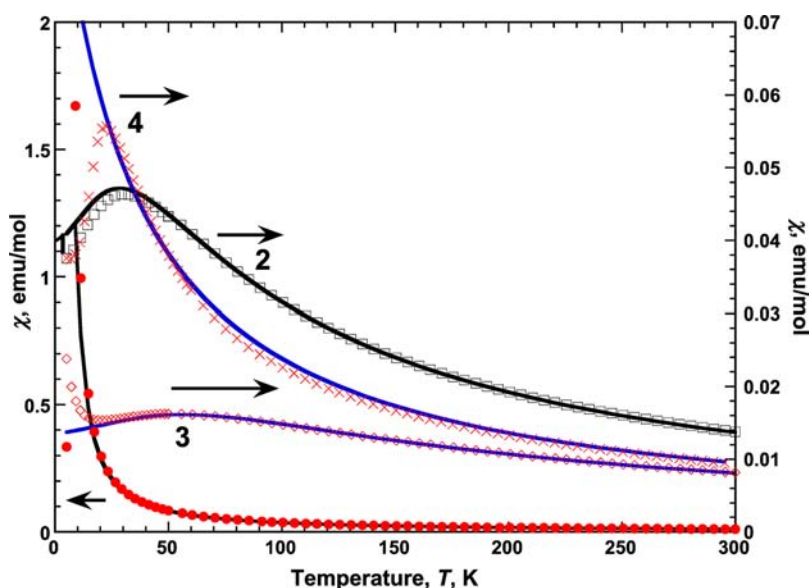


Figure 5. $\chi(T)$ for **1** (●), **2** (□), **3** (◆), and **4** (×), with fits to the Fisher chain expression, eq 2, (–) for **1**, **2**, and **3**, and a fit to the Curie–Weiss expression, eq 1, for **4** (–).

Table 6. Summary of Key Magnetic Parameters for Compounds **1** to **11**

	<i>S</i>	<i>g</i>	300 K $\chi T(T)_{\text{cal}}^b$	$\chi T(T)_{\text{obs}}^b$	emu Oe/mol	θ , K ^a	<i>D</i> / <i>k_B</i> , K	<i>J</i> / <i>k_B</i> , K	<i>T_{max}</i> $\chi(T)$, K	<i>T_{max}</i> $\chi(T)$, K	<i>T_c</i> , <i>T_{max}</i>	<i>d</i> (χT)/ <i>dT</i> , K
1	2	2.00	3.00, 3.43	3.00, 3.43		11		1.7	8	8		6
2	2.5	2.08	4.37, 4.13	4.37, 4.13		−43		−3.5	30	30		20
3	2	2.07	3.00, 2.44	3.00, 2.44		−118		−9.9	50	50		43
4	1.5	2.36	1.87, 2.69	1.87, 2.69		−40, −33 ^c			22	22		18
5	2.5	2.00	3.37, 2.76	3.37, 2.76					90	90		78
6	3	2.00	4.75, 4.80	4.75, 4.80					73	73		67
7	2	2.07	2.25, 2.05	2.25, 2.05		−50 ^e						
8	2	2.08, 2.06 ^d	3.00, 3.20	3.00, 3.20		−3.9 ^e , −1 ^d	−22 ^d					
9	2.5	2.00	4.37, 4.19	4.37, 4.19		−4.0 ^e						
10	1.5	2.31, 2.30 ^e	1.87, 2.46	1.87, 2.46		−3.0 ^e , −0.1 ^e	45 ^e					
11	1.5	2.70, 2.52 ^e	1.87, 3.26	1.87, 3.26		−20, −0.1 ^e	90 ^e					

^a($T^{-1} \rightarrow 0$). ^bSpin-only. ^cFrom a fit to eq 1. ^dFrom a fit to eq 4. ^eFrom a fit to eq 5.

lengths: 1.993(5) and 2.161(4) Å for **8**, 2.050(3) and 2.205(4) Å for **9**, and 1.963(5) and 2.120(5) Å for **10**. The M–O bond lengths are 2.115(7), 2.183(5), and 2.073(4) Å for **8** to **10**, respectively.

Compound **11** was determined to be $\text{Co}[\text{C}_4(\text{CN})_8]_2(\text{NCMe})_2$, and it is isostructural to the previously reported iron and manganese analogues.^{40,41} Its structure consists of an octahedral Co^{II} bound to $\mu_4\text{-}[\text{C}_4(\text{CN})_8]^{2-}$ forming 2-D layers with acetonitrile ligands coordinated above and below the plane.

Magnetic Properties. The temperature dependent magnetic susceptibility, χ , data were taken from 5 to 300 K, and are analyzed as $\chi(T)$, $\chi T(T)$, and $\chi^{-1}(T)$, and so forth, and key parameters are summarized in Table 5.

$M^{\text{II}}(\text{NCS})_2(\text{OCMe})_x$ [*M* = Fe (**1**), Mn (**2**), Cr (**3**), Co (**4**)]. The room temperature $\chi T(T)$ values for **1**, **2**, **3**, and **4** are 3.43, 4.13, 2.44, and 2.69 emuK/mol, respectively, indicating high spin M^{II} . The $\chi T(T)$ for **1** is constant on cooling until ~50 K when it increases and reaches a maximum of 15.5 emuK/mol at 8 K, before decreasing sharply until 5 K. The $\chi T(T)$ data of **2**, **3**, and **4** decrease constantly with decreasing temperature. A linear extrapolation of the $\chi^{-1}(T)$ above 200 K intercepts the temperature axis for the Weiss constant, θ , of 11, −43, −118, and −40 K for **1**, **2**, **3**, and **4**, respectively. The positive θ

for **1** indicates ferromagnetic coupling above 200 K, while $\theta < 0$ indicating antiferromagnetic coupling is observed for **2**, **3**, and **4**.

The $\chi(T)$ for **1**, **2**, **3**, and **4** can be fit to the Curie–Weiss expression, eq 1,

$$\chi \propto (T - \theta)^{-1} \quad (1)$$

but **1**, **2**, and **3** are better fit by the Fisher expression for 1-D chains,⁴³ which takes into account intrachain coupling (*J*/*k_B*) eq 2,

$$\chi_{\text{chain}} = \frac{Ng^2\mu_B S(S+1)}{3k_B T} \cdot \frac{1+u}{1-u} \quad \text{where}$$

$$u = \coth\left\{\frac{JS(S+1)}{k_B T}\right\} - \left\{\frac{k_B T}{JS(S+1)}\right\} \quad (2)$$

as seen for **2** in Figure 5. Compound **4** has $\theta = -33$ K. The *J*/*k_B* (*g*) for **1**, **2**, and **3**, are 1.7 (2.00), −3.5 (2.08), and −9.9 K (2.09), respectively, Table 6. In accord with the positive θ for **1**, **1** has a positive *J*/*k_B*, while **2** and **3** have negative *J*/*k_B* values suggesting antiferromagnetic coupling above the *T_c*.

Antiferromagnetic ordering is suggested by the peaks in $\chi(T)$ and $\chi'(T)$, at 8, 30, 50, and 22 K for **1–4**, respectively, and

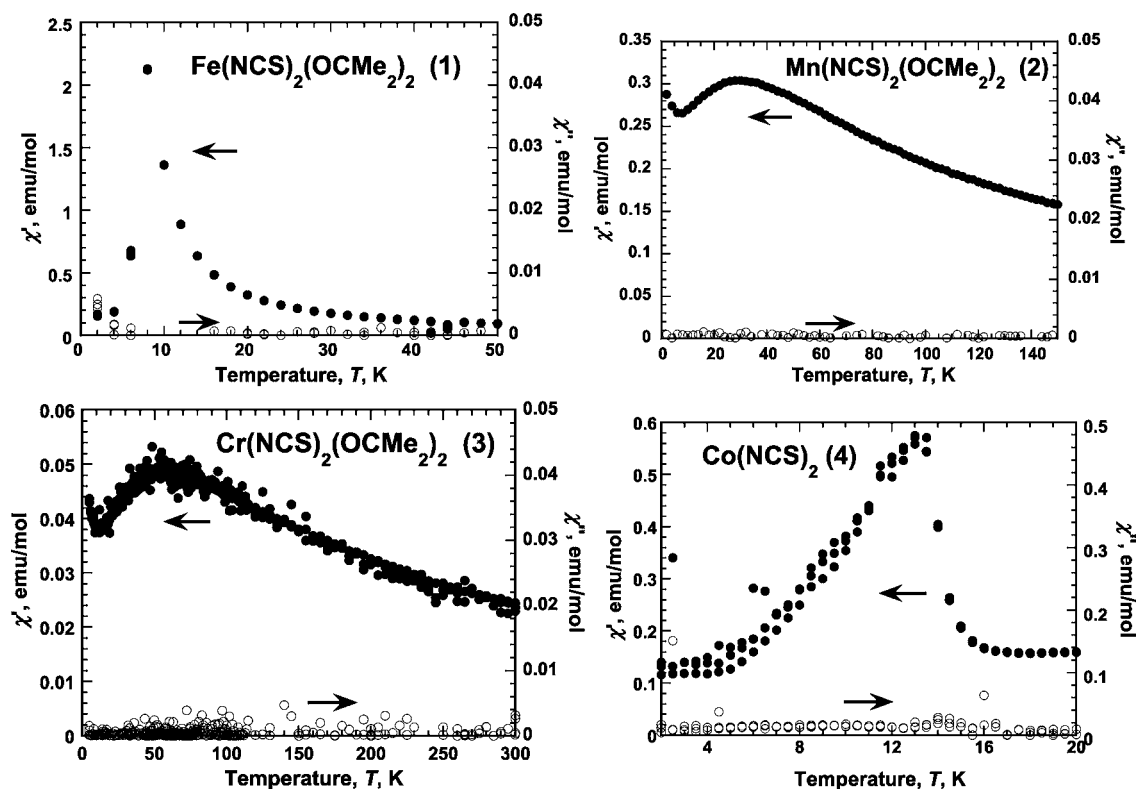


Figure 6. $\chi'(T)$ and $\chi''(T)$ for 1–4.

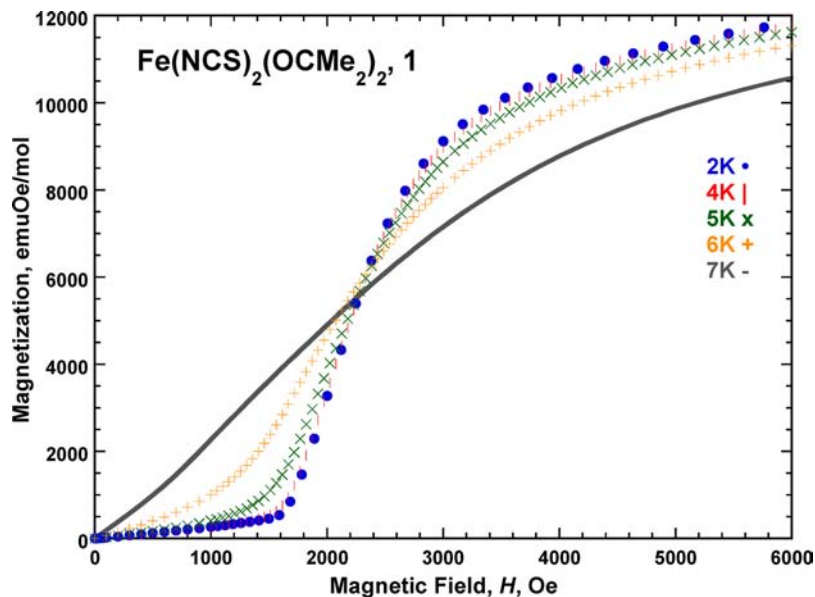


Figure 7. $M(H)$ at 2, 4, 5, 6 and 7 K for 1.

the lack of $\chi''(T)$ absorptions (Figure 6). The $\chi'(T)$ for 1–4 are frequency independent. The temperature at which the maximum in $\chi(T)$ occurs lies above T_{σ} ^{44,45} and T_c can be determined from the temperature at which the maximum in $d(\chi T)/dT$ occurs.^{46,47} The $d(\chi T)/dT$ maxima, T_{σ} occur at 6, 20, 43, and 18 K for 1, 2, 3, and 4, respectively. Similar ordering have been observed for $\text{Fe}(\text{NCS})_2(\text{py})_2$ ($T_c = 6.2$ K) and $\text{Mn}(\text{NCS})_2(\text{py})_2$ ($T_c = 23.5$ K),³⁶ which have similar 1-D chain moiety as compounds 1–3. The magnetic ordering occurs along the chain structure with small interaction between the chains.

Albeit antiferromagnetically ordered, 1 exhibits a field dependent magnetization below 8 K suggest metamagnetic-like⁴⁸ sigmoidal shape (Figure 7). The critical field, H_c is 900 Oe, determined by peak position of the dM/dH curve at 6 K. The sigmoid shape disappears above 6 K in accord with a 6 K T_c .

$M^{\text{II}}(\text{TCNE})[\text{C}_4(\text{CN})_8]_{1/2}$ [$M = \text{Fe}$ (5), Mn (6), Co (7)]. The magnetic behavior of $M(\text{TCNE})[\text{C}_4(\text{CN})_8]_{1/2}$ [$M = \text{Fe}^{23,33,34,49}$ (5), $\text{Mn}^{24,49,50}$ (6)] has been previously reported; however, the materials made via the reaction of $M(\text{NCS})(\text{OCMe}_2)_2$ and $[\text{TCNE}]^{*-}$ form materials with less impurities/defects, as evidenced by the low temperature magnetic data.

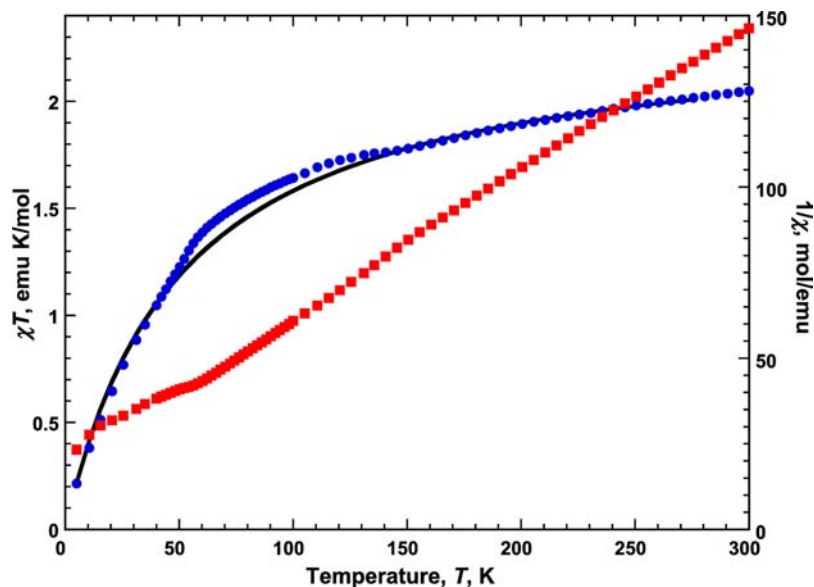


Figure 8. $\chi T(T)$ (●), $1/\chi$ (■), and the Curie–Weiss fitting expression (solid black line) with $g = 2.07$, and $\theta = -50$ K for 7.

Hence, the magnetic properties are of 5 and 6 made by this route are intrinsic, and are independently reported.⁵¹

The room temperature χT value for 7 is 2.05 emuK/mol, which are reduced from the spin-only value of 2.25 emuK/mol for one $S = 3/2$ Co(II) and one $S = 1/2$ [TCNE]^{•-} spin. This is attributed to antiferromagnetic coupling. Upon cooling $\chi T(T)$ decreases continuously from 300 to 5 K suggesting a paramagnetic system with antiferromagnetic coupling (Figure 8). The $\chi T(T)$ can be fit to the Curie–Weiss expression with $g = 2.07$, and $\theta = -50$ K suggesting strong antiferromagnetic coupling. The g value exceeds the spin-only value of 2.00, as Co^{II} is anisotropic, and is in the range of typical g values for Co^{II}.⁵² The small deviation below 50 and 140 K indicated more complex behavior, which is under further investigation. 7 can also be made from the reaction of Co^{II}(NCMe)₅Co^{II}(NCS)₄ and [TCNE]^{•-}, and exhibits a similar magnetic behavior.³² The lack of magnetic ordering is unexpected as isostructural 5 and 6 magnetically order. Nonetheless, it is in accord with that observed from the reaction of Co₂(CO)₈ and TCNE,⁵³ but is at variance from that observed from the reaction of CoI₂ and TCNE.³⁴ Further magnetic and theoretical studies are needed to understand the lack of ordering for Co(TCNE)[C₄(CN)₈]_{1/2}.

$M^{\text{II}}[\text{C}_4(\text{CN})_8](\text{O}_2\text{CMe}_2)_2$ [$M = \text{Fe}$ (8), Mn (9), Co (10)]. $M^{\text{II}}[\text{C}_4(\text{CN})_8](\text{O}_2\text{CMe}_2)_2$ [$M = \text{Fe}$ (8), Mn (9), Co (10)] was synthesized using acetone as the solvent, and the magnetic susceptibility indicated 8, 45, and 60 ppm ferromagnetic impurities, respectively, that are assumed to be iron (and cobalt). The corrected room temperature χT for 8, 9, and 10 are 3.20, 4.19, and 2.46 emuK/mol, respectively. The χT s for 8 and 9 are close to the spin-only values, but 10 significantly exceeds the spin only value of 1.87 emuK/mol, because of the anisotropic nature of Co^{II}.⁵² Upon cooling, $\chi T(T)$ for 8, 9, and 10 decrease continuously suggesting antiferromagnetic coupling (Figure 9). The $\chi T(T)$ can be fit to the Curie–Weiss expression, eq 1, with g -values of 2.08, 2.00, and 2.31, and θ -values of -3.9 , -4.0 , and -3.0 K, for 8, 9, and 10, respectively (Figure 9). Fits of $\chi T(T)$ to a single ion model that includes zero field splitting (D) gave a poorer fit for 9 using eq 3.^{54a} However, the fits for 8 (eq 4),^{54c} and 10 (eq 5)^{54b} have large D/k_B values of -22 and 45 K, with θ of -1.0 and -0.1 K,

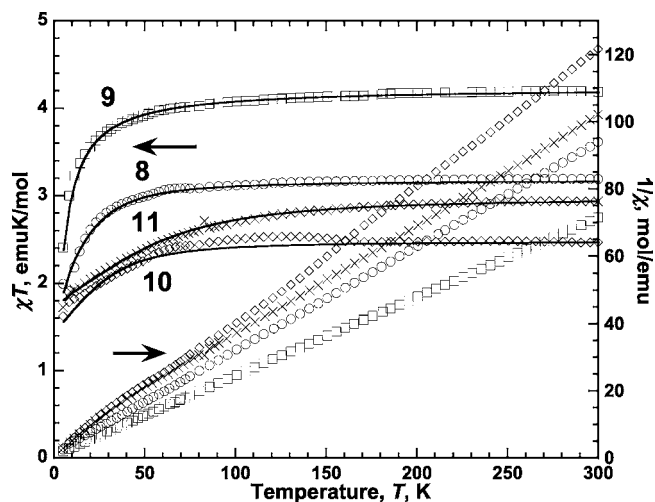


Figure 9. Corrected $\chi T(T)$ and $\chi^{-1}(T)$ for 8 (○), 9 (□), 10 (◇), and 11 (×), and fit to Curie–eq 1 for 8, eq 4 for 9, and eq 5 for 10 and 11 for the $\chi T(T)$ data.

and g of 2.06 and 2.30 for 8 and 10, respectively. These D -values are in agreement to the reported literature values of -57 K for K[tpa(mesityl)Fe^{II}] [tpa = tris(5-arylpyrrol-2-ylmethyl)amine],⁵⁵ and several octahedral Co^{II} complexes have D -values as high as 144 K.^{56,56}

$$\chi = \left[\frac{1}{12(T - \theta)} \frac{1 + 9e^{-2D/T} + 25e^{-6D/T}}{1 + e^{-2D/T} + e^{-6D/T}} \right] + \left[\frac{1}{6(T - \theta)} \frac{9 + \frac{8T}{D} - \frac{11T}{2D}e^{-2D/T} - \frac{5T}{2D}e^{-6D/T}}{1 + e^{-2D/T} + e^{-6D/T}} \right] \quad (3)$$

$$\chi = \left[\frac{1}{3(T - \theta)} \frac{2e^{-D/T} + 8e^{-4D/T}}{1 + 2e^{-D/T} + 2e^{-4D/T}} \right] + \left[\frac{2}{3(T - \theta)} \frac{\frac{6T}{D}(1 - e^{-D/T}) + \frac{4T}{3D}(e^{-D/T} - e^{-4D/T})}{1 + 2e^{-D/T} + 2e^{-4D/T}} \right] \quad (4)$$

$$\chi = \left[\frac{1}{3(T - \theta)} \frac{1 + 9e^{-2D/T}}{4(1 + e^{-2D/T})} \right] + \left[\frac{2}{3(T - \theta)} \frac{1 + \frac{3T}{4D}(1 - e^{-2D/T})}{1 + e^{-2D/T}} \right] \quad (5)$$

$\text{Co}^{\text{II}}[\text{C}_4(\text{CN})_8](\text{NCMe})_2$ (**11**). The room temperature χT for **11** is 3.26 emuK/mol that is comparable to **10** with both significantly exceeding the spin only value of 1.87 emuK/mol because of the anisotropic nature of Co^{II} .⁵² Upon cooling the $\chi T(T)$ for **11** decreases continuously to 50 K when it decreases more sharply suggesting antiferromagnetic coupling (Figure 9). The $\chi T(T)$ data can be fit to the Curie–Weiss expression, eq 1, with a g -value of 2.70, and $\theta = -20$ K suggesting antiferromagnetic coupling. A fit of $\chi T(T)$ to a single ion model that includes D , eq 5,^{54c} has $\theta = -0.1$ K, $g = 2.52$, and $D/k_B = 90$ K for **11** in accord with 131 K for $\text{Co}^{\text{II}}(\text{S-ATZ})_4\text{Cl}_2$ (AZT = 5-amino-1-*H*-tetrazole),^{56c} and several octahedral Co^{II} complexes have D -values as high as 144 K.⁵⁶

Compound **11** has a stronger magnetic coupling when compared to $\text{Fe}[\text{C}_4(\text{CN})_8](\text{NCMe})_2$ ($\theta = -13.3$ K).⁴⁰ The coupling constants for the acetonitrile containing compounds are 3 to 5 times larger than the acetone containing compounds (**8** to **10**). This difference could be attributed to the intralayer $\text{M}\cdots\text{M}$ distances, which are shorter for the acetonitrile containing compounds with respect to those possessing acetone.

CONCLUSION

Three new thiocyanate 1-D chain structured compounds of $\text{M}(\text{NCS})_2(\text{OCMe}_2)_2$ ($\text{M} = \text{Fe}, \text{Mn}, \text{Cr}$) composition were prepared and fully characterized. $\text{Fe}(\text{NCS})_2(\text{OCMe}_2)_2$ magnetically orders at 6 K and exhibits metamagnetic-like behavior. A new synthetic route to make $\text{Co}(\text{NCS})_2$ was identified and its structure was determined to be a 2-D layers with $\mu_{\text{N,S}}\text{-NCS}$ motif. These thiocyanate complexes react with $[\text{TCNE}]^{\bullet-}$ in dichloromethane to form $\text{M}(\text{TCNE})[\text{C}_4(\text{CN})_8]_{1/2}$, and in acetone to form $\text{M}[\text{C}_4(\text{CN})_8](\text{OCMe}_2)_2$ ($\text{M} = \text{Fe}, \text{Mn}, \text{Co}$). These compounds possess $\mu_4\text{-}[\text{C}_4(\text{CN})_8]^{2-}$. The magnetic behavior of $\text{M}(\text{TCNE})[\text{C}_4(\text{CN})_8]_{1/2}$ [$\text{M} = \text{Fe}$ (**5**), Mn (**6**)] has been previously reported; however, this reaction leads to materials with less impurities/defects, as evidenced by the low temperature magnetic data.⁵¹ $\text{Co}(\text{TCNE})[\text{C}_4(\text{CN})_8]_{1/2}$ exhibits paramagnetic properties with strong short-range antiferromagnetic coupling. $\text{M}[\text{C}_4(\text{CN})_8](\text{OCMe}_2)_2$ are paramagnetic.

ASSOCIATED CONTENT

Supporting Information

The observed PXRD as well as Rietveld fits for **4**, **7**, to **11**. The X-ray crystallographic CIF files for **1** to **6** and **8** to **11** (CCDC#806641, 806645, 806647, 876943–876948, respectively). This material is available free of charge via the Internet at <http://pubs.acs.org>.

AUTHOR INFORMATION

Corresponding Author

*E-mail: jsmiller@chem.utah.edu.

Notes

The authors declare no competing financial interest.

ACKNOWLEDGMENTS

We appreciate the continued partial support by the Department of Energy Division of Material Science (Grant DE-FG03-93ER45504) by E.S. and J.S.M. for the chemical synthesis, chemical characterization, and magnetic studies. Use of the National Synchrotron Light Source, Brookhaven National Laboratory, to execute powder X-ray diffraction studies by S.H.L. and P.W.S., was supported by the U.S. Department of Energy, Office of Basic Energy Sciences, under Contract No. DE-AC02-98CH10886.

REFERENCES

- (1) Bailey, R. A.; Kozak, S. L.; Michelsen, T. W.; Mills, W. N. *Coord. Chem. Rev.* **1971**, *6*, 407.
- (2) Burmeister, J. L. *Coord. Chem. Rev.* **1990**, *105*, 77.
- (3) Liu, T.; Zhu, J. Y. *Acta Crystallogr., Sect. E* **2007**, *63*, 2912.
- (4) Forster, D.; Goodgame, D. M. L. *J. Chem. Soc.* **1965**, 268.
- (5) (a) Defotis, G. C.; Barlowe, C. K.; Shangraw, W. R. *J. Mag. Mag. Mater.* **1986**, *54*, 1493. (b) Dockum, B. W.; Reiff, W. M. *Inorg. Chem.* **1982**, *21*, 391. (c) Flint, C. D.; Goodgame, M. J. *J. Chem. Soc. A.* **1970**, 442. (d) Nather, C.; Greve, J. *J. Solid State Chem.* **2003**, *176*, 259.
- (e) McElearney, J. N.; Balagot, L. L. *Phys. Rev. B* **1979**, *19*, 306.
- (6) Oki, H.; Kyuno, E.; Tsuchiya. *Bull. Chem. Soc. Jpn.* **1968**, *41*, 2357.
- (7) Faron, M. F.; Wojcicki, A. *Inorg. Chem.* **1965**, *4*, 1402.
- (8) Basolo, F.; Braddley, W. H.; Weidenbaum, K. J. *J. Am. Chem. Soc.* **1966**, *88*, 1576.
- (9) Jorgensen, C. K. *Inorg. Chem.* **1964**, *3*, 1201.
- (10) Sabatini, A.; Bertini, J. *Inorg. Chem.* **1965**, *4*, 1665.
- (11) Turco, A.; Pecile, C. *Nature* **1961**, *191*, 66.
- (12) Kabesova, M.; Boca, R.; Melnik, M.; Valigura, D.; Dunaj-Jurco, M. *Coord. Chem. Rev.* **1995**, *140*, 115.
- (13) (a) Chatt, J.; Duncanson, L. A. *Nature* **1956**, *178*, 997. (b) Chatt, J.; Duncanson, L. A.; Hart, F. A.; Owston, P. G. *Nature* **1958**, *181*, 43.
- (14) (a) Kivekas, R.; Pajunen, A.; Smolander, K. *Finn. Chem. Lett.* **1977**, 256. (b) Nelson, S. M.; Esho, F. S.; Drew, M. G. B. *J. Chem. Soc., Chem. Comm.* **1981**, 388.
- (15) (a) Wei, Z.; Li, H.; Ren, Z.; Lang, J.; Zhang, Y.; Sun, Z. *Dalton Trans.* **2009**, 3425. (b) Zhang, H.; Wang, X.; Zhu, H.; Xiao, W.; Zhang, K.; Teo, B. K. *Inorg. Chem.* **1999**, *38*, 886. (c) Crispini, A.; Errington, R. J.; Fisher, G. A.; Funke, F. J.; Norman, N. C.; Orpen, A. G.; Stratford, S. E.; Struve, O. *J. Chem. Soc., Dalton Trans.* **1994**, 1327.
- (16) Webster, O. W. personal communication. The reaction of KSCN and TCNE (1:1) in CH_2Cl_2 forms $[\text{TCNE}]^{\bullet-}$, as the IR data indicates the presence of $[\text{TCNE}]^{\bullet-}$ with two peaks at 2186 and 2148 cm^{-1} .
- (17) Miller, J. S. *Angew. Chem., Int. Ed.* **2006**, *45*, 2508.
- (18) Miller, J. S.; Epstein, A. J. *Angew. Chem., Int. Ed.* **1994**, *33*, 385.
- (19) Miller, J. S. *J. Chem. Soc. Rev.* **2011**, *40*, 3266.
- (20) Pokhodnya, K. I.; Bonner, M.; Her, J.-H.; Stephens, P. W.; Miller, J. S. *J. Am. Chem. Soc.* **2006**, *126*, 15592.
- (21) Buschmann, W. E.; Miller, J. S. *Chem.—Eur. J.* **1998**, *4*, 1731.
- (22) Webster, O.; Mahler, W.; Benson, R. E. *J. Org. Chem.* **1960**, *25*, 1470.
- (23) Her, J.-H.; Stephens, P. W.; Pokhodnya, K. I.; Bonner, M.; Miller, J. S. *Angew. Chem., Int. Ed.* **2007**, *46*, 1521.
- (24) Stone, K. H.; Stephens, P. W.; McConnell, A. C.; Shurdha, E.; Pokhodnya, J.-H.; Miller, J. S. *Adv. Mater.* **2010**, *22*, 2514.
- (25) Brandon, E. J.; Rittenberg, D. K.; Arif, A. M.; Miller, J. S. *Inorg. Chem.* **1998**, *37*, 3376.
- (26) Hoffmann, P.; Dedik, A. N.; Ensling, J.; Weinbruch, S.; Weber, S.; Sinner, T.; Gütlich, P.; Ortner, H. M. *J. Aerosol. Sci.* **1996**, *27*, 325.
- (27) (a) *Saint Plus*, v. 6.02; Bruker Analytical X-ray; Madison, WI, 1999. (b) Sheldrick, G. M. *SADABS*; University of Göttingen: Göttingen, Germany, 1996.

- (28) (a) Goldberg, I.; Krupitsky, H.; Stein, Z.; Hsiou, Y.; Strouse, C. E. *Supramol. Chem.* **1995**, *4*, 203. (b) Krupitsky, H.; Stein, Z.; Goldberg, I. *J. Inclusion Phenom. Mol. Recognit. Chem.* **1995**, *20*, 211. (c) Goldberg, I. *Mol. Cryst. Liq. Cryst.* **1996**, *278*, 767. (d) Byrn, M. P.; Curtis, C. J.; Hsiou, Y.; Kahn, S. I.; Sawin, P. A.; Tendick, S. K.; Terzis, A.; Strouse, C. E. *J. Am. Chem. Soc.* **1993**, *115*, 9480. Byrn, M. P.; Curtis, C. J.; Hsiou, Y.; Khan, S. I.; Sawin, P. A.; Terzis, A.; Strouse, C. E. In *Comprehensive Supramolecular Chemistry*; Atwood, J. L., Davies, J. E. D., MacNicol, D. D., Vogtle, F., Eds.; **1996**; Vol. 6, p 715.
- (29) TOPAS V3: General profile and structure analysis software for powder diffraction data, User's Manual; Bruker AXS: Karlsruhe, Germany, 2005.
- (30) Coelho, A. A. *J. Appl. Crystallogr.* **2000**, *33*, 899.
- (31) TOPAS-Academic is available at www.topas-academic.net.
- (32) Shurdha, E.; Moore, C. E.; Rheingold, A. L.; Miller, J. S. *Inorg. Chem.* **2011**, *50*, 10546.
- (33) Pokhodnya, K. I.; Petersen, N.; Miller, J. S. *Inorg. Chem.* **2002**, *41*, 1996.
- (34) Zhang, J.; Enslin, J.; Ksenofontov, V.; Gülich, P.; Epstein, A. J.; Miller, J. S. *Angew. Chem., Int. Ed.* **1998**, *37*, 657.
- (35) (a) Gower, M. L.; Crowley, J. *Dalton Trans.* **2010**, *39*, 2371. (b) Castellari, C.; Feroci, G.; Ottani, S. *Acta Crystallogr., Sect. C: Cryst. Struct. Commun.* **1999**, *55*, 907. (c) Nicholas, K. M.; Khan, M. A. *Inorg. Chem.* **1987**, *26*, 1633. (d) Werner, H.; Munch, G.; Laubender, M. *Inorg. Chim. Acta* **2005**, *358*, 1510. (e) Maekawa, M.; Kayanuma, Y.; Nabei, A.; Kuroda-Sowa, T.; Suenaga, Y.; Munakata, M. *Inorg. Chim. Acta* **2005**, *358*, 1313. (f) Margraf, G.; Bats, J. W.; Wagner, M.; Lerner, H. W. *Inorg. Chim. Acta* **2005**, *358*, 1193. (g) Windmuller, B.; Nurnberg, O.; Wolf, J.; Werner, H. *Eur. J. Inorg. Chem.* **1999**, 613. (h) Cotton, F. A.; Hillard, E. A.; Liu, C. Y.; Murillo, C. A.; Wang, W.; Wang, X. *Inorg. Chim. Acta* **2002**, *337*, 233. (i) Gandhi, B. A.; Green, O.; Burstyn, J. N. *Inorg. Chem.* **2007**, *46*, 3816. (j) Dikarev, E. V.; Andreini, K. W.; Petrukhina, M. A. *Inorg. Chem.* **2004**, *43*, 3219. (k) Gambarotta, S.; Pasquali, M.; Floriani, C.; Villa, A. C.; Guastini, C. *Inorg. Chem.* **1981**, *20*, 1173. (l) Lindsay, A. J.; Wilkinson, G.; Motevalli, M.; Hursthouse, M. B. *J. Chem. Soc., Dalton Trans.* **1985**, 2321. (m) Salem, H.; Shimon, L. J. W.; Leitus, G.; Weiner, L.; Milstein, D. *Organometallics* **2008**, *27*, 2293.
- (36) Boeckmann, J.; Näther, C. *Polyhedron* **2012**, *31*, 587. Boeckmann, J.; Näther, C. *Dalton Trans.* **2010**, *39*, 11019.
- (37) (a) Dockum, B. W.; Reiff, W. M. *Inorg. Chem.* **1982**, *21*, 391. (b) Dockum, B. W.; Reiff, W. M. *Inorg. Chem.* **1982**, *21*, 1406. (c) Lapidus, S. H.; Stephens, P. W.; Shurdha, E.; DaSilva, J. G.; Miller, J. S. *Polyhedron* **2012**, in press.
- (38) Dubler, E.; Reller, A.; Oswald, H. R. *Z. Kristallogr.* **1982**, *161*, 265.
- (39) Boeckmann, J.; Nathar, C. *Polyhedron* **2012**, *31*, 587.
- (40) Zhang, J.; Liable-Sands, L. M.; Rheingold, A. L.; Del Sesto, R. E.; Gordon, D. C.; Burkhart, B. M.; Miller, J. S. *Chem. Commun.* **1998**, 1385.
- (41) Pokhodnya, K. I.; Bonner, M. I.; DiPasquale, A. G.; Rheingold, A. L.; Miller, J. S. *Chem.—Eur. J.* **2008**, *14*, 714.
- (42) Wang, G.; Slebodnick, C.; Yee, G. T. *Inorg. Chem.* **2007**, *46*, 9641.
- (43) (a) Kahn, O. *Molecular Magnetism*; VCH: Weinheim, Germany, 1993; p 275. (b) Chen, Z.; Jiang, C.; Yan, W.; Liang, F.; Batten, S. R. *Inorg. Chem.* **2009**, *48*, 4674.
- (44) Fisher, M. E. *Philos. Mag.* **1962**, *7*, 1731.
- (45) Ashcroft, N. W.; Mermin, N. D. *Solid State Physics*; W. B. Saunders and Co.: Philadelphia, PA, 1976; p 701 ff.
- (46) Aharen, T.; Greedan, J. E.; Ning, F.; Imai, T.; Michaelis, V.; S.; Zhou, H.; Wiebe, C. R.; Cranswick, L. M. D. *Phys. Rev. B* **2009**, *80*, 134423.
- (47) Cage, B.; Nguyen, B.; Dalal, N. *Solid State Commun.* **2001**, *119*, 597.
- (48) Stryjewski, E.; Giordano, N. *Adv. Phys.* **1977**, *26*, 487.
- (49) Girtu, M. A.; Wynn, C. M.; Zhang, J.; Miller, J. S.; Epstein, A. J. *Phys. Rev. B* **2000**, *61*, 492.
- (50) Girtu, M. A.; Wynn, C. M.; Zhang, J.; Miller, J. S.; Epstein, A. *Phys. Rev.* **1998**, *B58*, 8508.
- (51) McConnell, A. C.; Shurdha, E.; Bell, J. D.; Miller, J. S. *J. Phys. Chem. C* **2012**, *16*, 0000.
- (52) Carlin, R. L. *Magnetochemistry*; Springer-Verlag: New York, 1986; p 66, p 155 ff, p 301 ff.
- (53) Pokhodnya, K. I.; Burtman, V.; Epstein, A. J.; Raebiger, J. W.; Miller, J. S. *Adv. Mater.* **2003**, *15*, 1211.
- (54) (a) Kahn, O. *Molecular Magnetism*; VCH: Weinheim, Germany, 1993; p 23; (b) Kahn, O. *Molecular Magnetism*; VCH: Weinheim, Germany, 1993; p 21. (c) O'Connor, C. *Prog. Inorg. Chem.* **1982**, *29*, 203.
- (55) Freedman, D. E.; Harman, W. H.; Harris, T. D.; Long, G. J.; Chang, C. J.; Long, J. R. *J. Am. Chem. Soc.* **2010**, *122*, 1224.
- (56) (a) Boca, R.; Titus, J. *Inorg. Chem.* **2011**, *50*, 11838. (b) Boca, R. *Coord. Chem. Rev.* **2004**, *248*, 757. (c) Zhao, F.; Che, Y.; Zheng, J. *Inorg. Chem.* **2012**, *51*, 4862.